

## Polarization-dependent electron affinity of $\text{LiNbO}_3$ surfaces

W.-C. Yang, B. J. Rodriguez, A. Gruverman, and R. J. Nemanich<sup>a)</sup>

*Department of Physics, and Department of Materials Science and Engineering, North Carolina State University, Raleigh, North Carolina 27695-8202*

(Received 10 May 2004; accepted 7 July 2004)

Polar surfaces of a ferroelectric  $\text{LiNbO}_3$  crystal with periodically poled domains are explored using UV-photoelectron emission microscopy (PEEM). Compared with the positive domains (domains with positive surface polarization charges), a higher photoelectric yield is found from the negative domains (domains with negative surface polarization charges), indicating a lower photothreshold and a corresponding lower electron affinity. The photon-energy-dependent contrast in the PEEM images of the surfaces indicates that the photothreshold of the negative domains is  $\sim 4.6$  eV while that of the positive domains is greater than  $\sim 6.2$  eV. We propose that the threshold difference between the opposite domains can be attributed to a variation of the electron affinity due to opposite surface dipoles induced by surface adsorbates. © 2004 American Institute of Physics.

[DOI: 10.1063/1.1790604]

Ferroelectric materials have unique surface properties associated with the spontaneous polarization, which induces macroscopic polarization charges at the surface.<sup>1</sup> To obtain an energetically stable state, the surface polarization charges are screened by the formation of a space-charge layer in the vicinity of the surface (internal screening), and/or by the surface adsorption of charged molecules (external screening). The relative contribution of the internal and external mechanisms to polarization screening can modify the energy bands at the surface. The internal electric field induced by the space-charge layer leads to surface band bending,<sup>1</sup> while surface adsorption can give rise to a variation in the surface electron affinity as well as band bending.<sup>2</sup> Thus, the surface electronic properties of ferroelectric materials are controlled by the orientation of the spontaneous polarization, which determines the sign of the polarization bound charge and the internal and external screening charges.

Recently, precise control of ferroelectric domains has become a crucial issue for many applications. In particular, an approach to the self-assembly of complex nanostructures is based on manipulating atomic polarization in ferroelectric substrates.<sup>3</sup> Detailed information about local polarization, charge distribution, and surface potential of a ferroelectric surface is necessary to control local electronic structures and chemical reactivity.

The surface properties of ferroelectric domains with different polarities have been characterized by scanning probe microscopy (SPM)-based techniques such as piezoresponse force microscopy (PFM),<sup>4</sup> electrostatic force microscopy (EFM),<sup>5</sup> and scanning kelvin probe microscopy (SKPM).<sup>6</sup> However, as Kalinin and Bonnell pointed out,<sup>6</sup> the extraction of the intrinsic material properties from the measurements and the interpretation of the domain contrast mechanism in many variants of SPM are unclear due to the complexity of the tip-surface interactions. Alternatively, scanning electron microscopy (SEM) has been employed for the observation of ferroelectric domain structures.<sup>7,8</sup> The SEM domain contrast was ascribed to asymmetric secondary electron emission

from opposite domains due to the pyroelectric potential difference induced by electron beam heating<sup>7</sup> or due to a work function difference induced by surface adsorption.<sup>8</sup> It is worth noting that different groups observed opposite SEM contrast for domains of the same polarity and that the proposed models did not reconcile these contradictory results.

To better understand the mechanism of domain contrast and explore the effect of domain polarity on surface electronic properties, we employ UV-photoelectron emission microscopy (UV-PEEM) for domain imaging of lithium niobate surfaces. Recently, we demonstrated that PEEM is capable of imaging of Ga- and N-face regions of cleaned GaN films.<sup>9</sup> The contrast was due to the enhanced emission from the N-face regions, which was attributed to the photoemission of electrons in the conduction band at the surface induced by band bending. Similarly, a variation in electron affinity and/or band bending could give rise to ferroelectric domain contrast in PEEM. The goal of this study is to establish how these effects are manifested in PEEM images of ferroelectric surfaces with opposite polarization. In particular, with tunable UV-free electron laser (FEL) excitation, we determine the photothreshold and the variation in the electron affinity of different polar regions.

In this work, we used a periodically poled lithium niobate (PPLN) single crystal with a periodicity of patterned domains of  $\sim 6.8$   $\mu\text{m}$ . Below the 1210 °C Curie temperature, the ferroelectric lithium niobate (LNO) exhibits a hexagonal crystal structure with polarization along the  $c$  axis, which arises due to displacement of positive charges ( $\text{Li}^+$  and  $\text{Nb}^{5+}$ ) with respect to oxygen atom positions.<sup>10</sup> The periodic domain structure was fabricated by lithography and electric poling on the original  $+c$  face of congruent (0001) LNO. The sample size was  $10 \times 10 \times 0.2$  mm<sup>3</sup>. The domain observations were performed in an UV-PEEM system (Elmitech) with a base pressure  $< 2 \times 10^{-10}$  Torr. The photoelectrons were excited with spontaneous emission from the tunable UV - FEL at Duke University. The PEEM images were obtained with photon energies from 4–6.2 eV with an energy full width at half maximum of  $\sim 0.1$  eV.<sup>7</sup> To verify domain polarity, complementary PFM imaging of the sample has been performed.

<sup>a)</sup> Author to whom correspondence should be addressed; electronic mail: Robert\_Nemanich@ncsu.edu

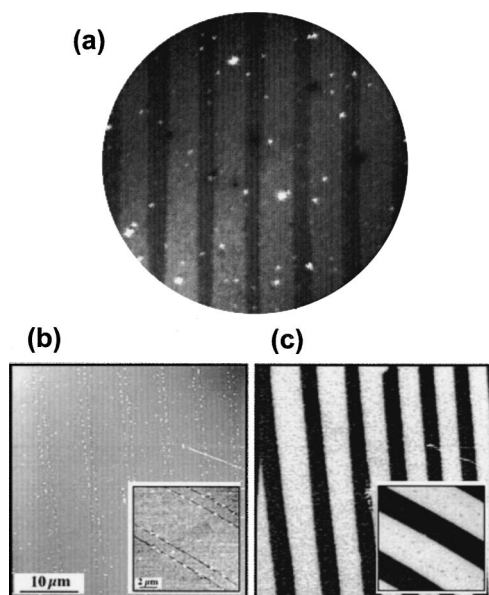


FIG. 1. (a) PEEM, (b) AFM, and (c) PFM images of PPLN. The fields of view are 40  $\mu\text{m}$ . Insets in (b) and (c) are  $10 \times 10 \mu\text{m}^2$  and all images were obtained from the same surface. The PEEM image was obtained with a photon energy of 5.1 eV. In (b), the double lines remained at the negative domain boundary regions after the lithography process. In (c), the PFM image obtained from the same region of the AFM image shows that the marked regions are negative domains which are brighter and wider than the positive domains.

Figure 1(a) displays a PEEM image of the surfaces of the as-received PPLN sample. The brightness contrast between antiparallel domains is apparent. The wider domains ( $\sim 4.5 \mu\text{m}$ ) are relatively brighter than the narrower domains ( $\sim 2.3 \mu\text{m}$ ). The bright spots in the image may be dust particles or other foreign materials. Through comparison of the AFM, PFM, and PEEM images shown in Fig. 1, we could identify the polarity of the domains. The bright regions in the PEEM image are recognized as negative domains (domains with negative surface polarization charges), while the darker regions are positive domains (domains with positive surface polarization charges); indicating relatively intense electron emission from the surface of the negative domains. The topographic AFM image [Fig. 1(b)] shows a similar morphology for both domains, which suggests that the PEEM domain contrast is independent of surface topography. PFM analysis [Fig. 1(c)] of the periodic domain pattern confirmed that the wider stripes correspond to the negative domains.

To explore the surface electronic properties of each domain, PEEM images were obtained with photon energies from 4–6.2 eV in steps of 0.1 eV (Fig. 2). For photon energies below 4.5 eV, domain contrast was not detected [Fig. 2(a)]. However, for photon energies greater than 4.6 eV, emission from the negative domains was observed, which thus allowed us to differentiate between the opposite domains [Fig. 2(b)]. As the photon energy was increased from 4.6 eV, the emission from the negative domains increased, leading to enhanced contrast [Fig. 2(c)]. However, at 6.2 eV the emission from the positive domain became more significant, and the emission contrast was relatively reduced [Fig. 2(d)]. From the results, we deduce that the electron photothreshold of the negative domains is  $\sim 4.6$  eV while that of the positive domains is greater than 6.2 eV.

There have been several other studies that explored the photothreshold of polar LNO surfaces. In studies of undoped

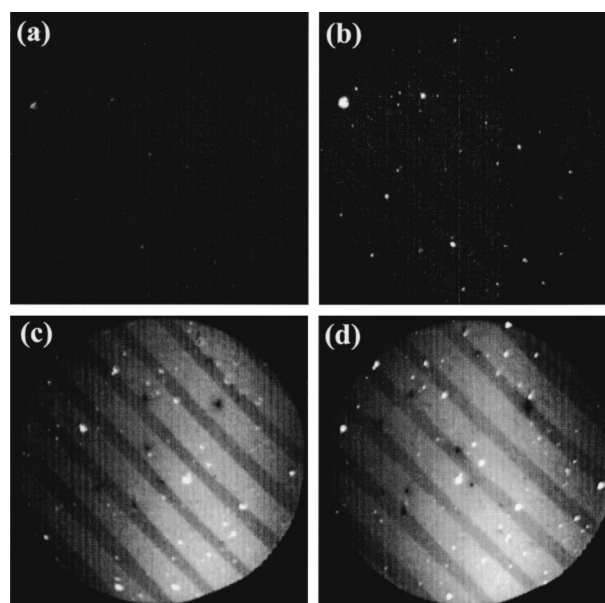


FIG. 2. PEEM images of PPLN obtained with photon energies of (a) 4.5 eV, (b) 4.6 eV, (c) 5.2 eV, and (d) 6.2 eV, respectively. The field of view is 10  $\mu\text{m}$ .

LNO surfaces cleaned by vacuum annealing between 300 and 900  $^{\circ}\text{C}$ , Akhayan and Brozdnicenko<sup>11</sup> deduced that the photothreshold was independent of polarity, and they found an electron affinity of  $\sim 1.1$  eV. They did find a variation in the emission intensity and the subthreshold emission for the different polarity surfaces. Boikova and Rosenman<sup>12</sup> measured the emission from Fe-doped LNO. Their results showed emission beginning at an excitation energy of  $\sim 4.0$  eV, and differences in the emission from the different polar surfaces were attributed to band-bending effects.

In UV-PEEM the image contrast originates from local variation in the photoelectric yield, which is usually related to the photoelectric threshold. For an intrinsic semiconductor with flat bands at the surface, the photothreshold,  $E_{\text{th}}$ , is equal to the sum of the band gap,  $E_g$ , and the electron affinity,  $\chi_s$ .<sup>13</sup> In contrast, for an actual semiconductor surface, the threshold is dependent on the band structure at the surface, which can vary with the doping and the band bending.<sup>9</sup> It is noted that due to its  $E_g$  of 3.9 eV, LNO would be considered as a wide band-gap ferroelectric semiconductor.<sup>12</sup> Thus, to understand the origin of the PEEM polarity contrast mechanism of the ferroelectric domains, it is necessary to consider the effects of band bending and electron affinity.

If the polarization charges are internally screened by a space-charge layer, band bending is generated in the space-charge region near the surfaces. Unfortunately, we have no direct measurement of the band bending in the near surface region of these LNO samples. Generally, the width of a space-charge layer in a semiconductor with a low concentration of charge carriers is  $> \sim 100$  nm while for a photon energy lower than 10 eV the electron mean free path of LNO is  $< 5$  nm.<sup>14</sup> Since our LNO sample is undoped, it may be reasonable to assume that any band bending that exists will occur over a length scale that will be large compared to the length scale for UV absorption and/or electron emission. Thus, the band-bending effects on the emission from the undoped LNO is negligible in the PEEM measurements.

We next consider the variation in electron affinity at each domain surface induced by the external screening. The elec-

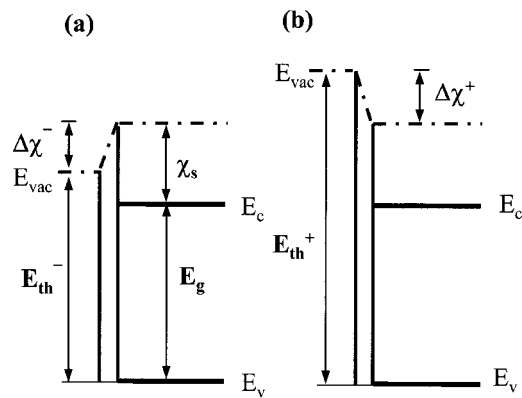


FIG. 3. Energy-band diagrams of adsorbate-covered LiNbO<sub>3</sub> surfaces for (a) negative and (b) positive domains. The quantities  $\chi_s$ ,  $E_g$ ,  $E_{th}$ , and  $\Delta\chi$  are the surface electron affinity, band gap, photothreshold, and electron affinity variation due to surface adsorption, respectively. Superscripts represent the quantities of negative (–) and positive (+) domain. The arrows represent the orientations of the spontaneous polarization,  $P_s$ .

tron affinity at a semiconductor surface is a function of the surface dipole induced by various surface effects such as surface termination, surface reconstruction, surface orientation, local stoichiometry changes, atomic steps, and adsorbates.<sup>2,15</sup> We are suggesting that for a ferroelectric semiconductor, the screening of the polarization charges by adsorption of charged molecules or ions on a surface (external screening) will give rise to an additional surface dipole<sup>1,6,16,17</sup> and result in a variation in the electron affinity. This effect is modeled schematically in Fig. 3 for the two polar LNO surfaces. The change of the electron affinity can be estimated by the following relation:

$$\Delta\chi = \frac{e^2 N \delta}{\epsilon} = \frac{epN}{\epsilon},$$

where  $N$  is the number of ions per unit surface area,  $\epsilon$  is dielectric constant of the dipole layer, and  $\delta$  is the effective distance between the charge centers (dipole  $p=e\delta$ ). The adsorbed species will be determined by the surface polarity of the ferroelectric. For a negative domain, positive ions would be adsorbed, and the electron affinity should decrease ( $\Delta\chi < 0$ ) while for a positive domain, negative ions would be adsorbed, and the affinity should increase ( $\Delta\chi > 0$ ). As shown in Fig. 3, the electron affinity variation would lead to a variation in the photothreshold at the different polar domains. For the negative domain, the photothreshold decreases by  $\Delta\chi^-$  (where  $E_{th}^- = E_g + \chi_s - \Delta\chi^-$ ) while for the positive domain the photothreshold increases by  $\Delta\chi^+$  (where  $E_{th}^+ = E_g + \chi_s + \Delta\chi^+$ ). Consequently, the relatively bright emission from the negative domains of the LNO is attributed to a reduction of the photothreshold due to surface adsorption of positive ions, and the PEEM polarity contrast of the LNO is attributed to the variation in the electron affinity induced by the surface adsorption of both the positive and negative domains. Thus, in the absence of external screening of the polarization charges, for an ideal, cleaned LNO surface, the PEEM polarity contrast would not be detected since the electron affinity would be same for both domains ( $\Delta\chi^+ = \Delta\chi^- = 0$ ).

The PEEM measurements shown in Fig. 2 indicate that the threshold difference between positive and negative do-

main of the air exposed surface is greater than  $\sim 1.6$  eV, which would correspond to  $\Delta\chi^- + \Delta\chi^+$ . If we assume that the polarization charges are completely screened by the surface adsorption, we can estimate  $N \sim P_s/q$  from the spontaneous polarization,  $P_s$ . For LNO,  $N \sim 4.4 \times 10^{14}/\text{cm}^2$  [ $P_s = 70 \times 10^{-6} \text{C}/\text{cm}^2$  (Ref. 12)]. If we assume a surface dipole layer with a charge separation distance,  $\delta$ , of 0.3 nm and a dielectric constant,  $\epsilon$  of 31 (LNO), the  $\Delta\chi$  at each domain surface will be  $\sim 0.8$  eV. This value is an estimate because the dielectric constant of the dipole layer is an ill-defined property since the dipole layer is not a bulk entity. However, this estimated value is consistent with our PEEM measurements. In addition, assuming  $\Delta\chi$  of  $\sim 0.8$  eV for each domain, we can deduce that the value of  $\chi_s$  is  $\sim 1.5$  eV ( $\chi_s = E_{th}^+ - E_g - \Delta\chi^+$ ). Photoemission studies of cleaned LNO surfaces with no adsorbates have yielded a value of electron affinity of  $\sim 1.1$  eV,<sup>11</sup> which is close to our results.

In summary, we have used UV-PEEM to image periodically poled domains in lithium niobate. Polarity contrast was observed between the positive and negative domains with more intense emission from the negative domains. We propose that the threshold difference is caused by variations in surface electron affinity associated with surface dipole layers formed by surface adsorbates.

The authors gratefully acknowledge the Duke Free Electron Laser Laboratory for access to the OK-4 free electron laser. Useful discussion with Professor G. Rosenman is gratefully acknowledged. This work was supported by grants through the MFEL program administered through the AFOSR, the Office of Naval Research MURI on Polarization Electronics Contract No. N00014-99-1-0729, and the NSF under Grant No. DMR 0235632.

<sup>1</sup>V. M. Fridkin, *Ferroelectric Semiconductors* (Consultants Bureau, New York, 1980).

<sup>2</sup>H. Luth, *Surfaces and Interfaces of Solids*, 2nd ed. (Springer, Berlin, 1993).

<sup>3</sup>S. V. Kalinin, D. A. Bonnell, T. Alvarez, X. Lei, Z. Hu, and J. H. Ferris, *Nano Lett.* **2**, 589 (2002).

<sup>4</sup>A. Gruverman, O. Aueiello, and H. Tokumoto, *Annu. Rev. Mater. Sci.* **28**, 101 (1998).

<sup>5</sup>R. Lüthi, H. Haefke, K.-P. Meyer, E. Meyer, L. Howald, and H.-J. Güntherodt, *J. Appl. Phys.* **74**, 7461 (1993).

<sup>6</sup>S. V. Kalinin and D. A. Bonnell, *Phys. Rev. B* **63**, 125411 (2001).

<sup>7</sup>G. Rosenman, A. Skliar, I. Lareah, N. Angert, M. Tseitlin, and M. Roth, *Phys. Rev. B* **54**, 6222 (1996).

<sup>8</sup>R. Le Bihan, *Ferroelectrics* **97**, 19 (1989).

<sup>9</sup>W.-C. Yang, B. J. Rodriguez, M. Park, R. J. Nemanich, O. Ambacher, and V. Cimalla, *J. Appl. Phys.* **94**, 5720 (2003).

<sup>10</sup>S. C. Abrahams, H. J. Levinstein, and J. M. Reddy, *J. Phys. Chem. Solids*, **27**, 1019 (1966).

<sup>11</sup>A. A. Akhayan and A. N. Brozdnicenko, *Sov. Phys. Solid State* **25**, 1990 (1983); A. A. Akhayan, A. N. Brozdnicenko, and E. V. Bursian, *ibid.* **20**, 912 (1978).

<sup>12</sup>E. I. Boikova and G. I. Rosenman, *Sov. Phys. Solid State* **20**, 1976 (1978); G. I. Rosenman, E. I. Boikova, and Y. L. Chepelev, *Phys. Status Solidi A* **69**, k173 (1982).

<sup>13</sup>D. Cahen and A. Kahn, *Adv. Mater. (Weinheim, Ger.)* **15**, 271 (2003).

<sup>14</sup>P. Steiner and H. Hochst, *Z. Phys. B* **35**, 51 (1979).

<sup>15</sup>R. J. Nemanich, *GaN and Related Semiconductors*, edited by J. H. Edgar, S. Strite, I. Akasaki, H. Amano, and C. Wetzel (INSPEC, London, 1999), p. 98.

<sup>16</sup>S. V. Kalinin, C. Y. Johnson, and D. A. Bonnell, *J. Appl. Phys.* **91**, 3816 (2002).

<sup>17</sup>M. M. Shvebelman, A. G. Agronin, R. P. Urenski, Y. Rosenwaks, and G. I. Rosenman, *Nano Lett.*, **2**, 455 (2002).